Organic & Biomolecular Chemistry

ROYAL SOCIETY OF CHEMISTRY

REVIEW

View Article Online
View Journal

Cite this: DOI: 10.1039/d6ob00736h

Imine bond protection by supramolecular encapsulation

Kejia Shi † and Bradley D. Smith *†

The imine bond (Schiff base) is ubiquitous in chemistry, biochemistry, and materials science, even though it is susceptible to hydrolysis in aqueous environments. Nature protects reactive imines by molecular encapsulation within hydrophobic protein binding pockets. This review summarizes the various synthetic supramolecular strategies that have been developed to stabilize a C=N bond and protect it from hydrolysis. Early biomimetic approaches investigated self-inclusion host systems, such as deep cavitands and pillar[5]arenes, that were equipped with anchored functional groups to form stabilized imines. Other approaches used a water-soluble metallocage or cucurbit[7]uril as a host molecule to capture and protect an iminium cation or Schiff base. A recent study showed that a self-assembled capsule can sequester the two reactants (amine and carbonyl) from water and promote imine formation inside the capsule hydrophobic interior. Adding a high-affinity guest to the supramolecular complex displaces the encapsulated imine, which then hydrolyzes in the surrounding water. Future applications of this supramolecular technology are expected in prodrug delivery, responsive materials, and supramolecular catalysis.

Received 8th May 2026,
Accepted 3rd June 2026

DOI: 10.1039/d6ob00736h

rsc.li/obc

Introduction to imine structure and chemistry

Schiff bases are part of the broader imine family of functional groups and they are commonly investigated in organic chemistry, metal coordination chemistry, materials science, and medicinal chemistry.[1–3] Schiff bases are made by condensing aldehydes or ketones with primary amines to make aldimines or ketimines, whereas carbonyl condensation with a secondary amine generates a permanently charged iminium cation (Fig. 1). These equilibria are highly sensitive to the solution pH.[4,5] From the perspective of Schiff base hydrolysis, the reaction is fastest in acid (typically around pH 4) where the imine nitrogen is protonated and nucleophilic attack by water generates an unstable hemiaminal intermediate that subsequently converts into the separate carbonyl and amine components.[6] The reversibility of imine formation has been exploited as an error-correcting, self-assembly method to synthesize complex but thermodynamically stable molecules such as molecular cages, knots, macrocycles, and polymer networks.[7–9] Furthermore,

Department of Chemistry and Biochemistry, University of Notre Dame, 251 Nieuwland Science Hall, Notre Dame, Indiana 46556, USA.
E-mail: smith.115@nd.edu
† Both authors contributed equally to this review article.

Kejia Shi

Kejia Shi received his B.S. degree from Fudan University. He joined Prof. Smith's research group at the University of Notre Dame in 2021, and was awarded his Ph.D. in 2026. His graduate research focused on supramolecular chemistry and optical sensors.

Bradley D. Smith

Bradley D. Smith is the Emil T. Hofman Professor of Science in the Department of Chemistry and Biochemistry at the University of Notre Dame. He designs smart molecules for imaging, therapy, and health and many projects are approached using the rules of supramolecular chemistry.

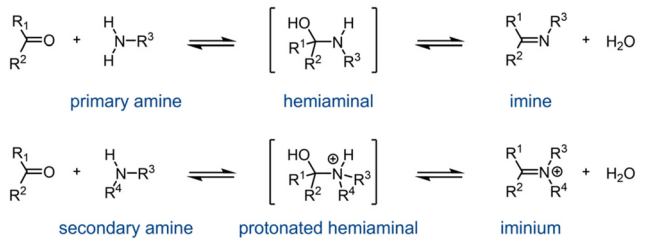

Fig. 1 Formation and hydrolysis of an imine (Schiff base) or iminium cation.

imine reversion has been used as a structural design element within advanced materials that exhibit adaptive, responsive, or processable properties.[10] The reversibility of imine formation also makes it attractive for dynamic covalent chemistry where one research goal is to self-assemble imine-containing building blocks within the binding pocket of a biomacromolecule.[11] Imine linkers are also attractive for various forms of bioconjugation chemistry, however, the hydrolytic susceptibility is often a practical limitation. Synthetic chemists have confronted this challenge by developing imine structures with *ortho*-substituted hydroxyl or boronic acids that can form stabilizing interactions with the imine nitrogen atom.[12,13] Another synthetic method to stabilize an imine linkage is to create amphiphilic molecules that self-assemble in aqueous solution to form aggregates, such as micelles or vesicles, with the imine bond spatially located in the hydrophobic core away from the bulk water.[14,15] These different synthetic strategies for imine stabi-

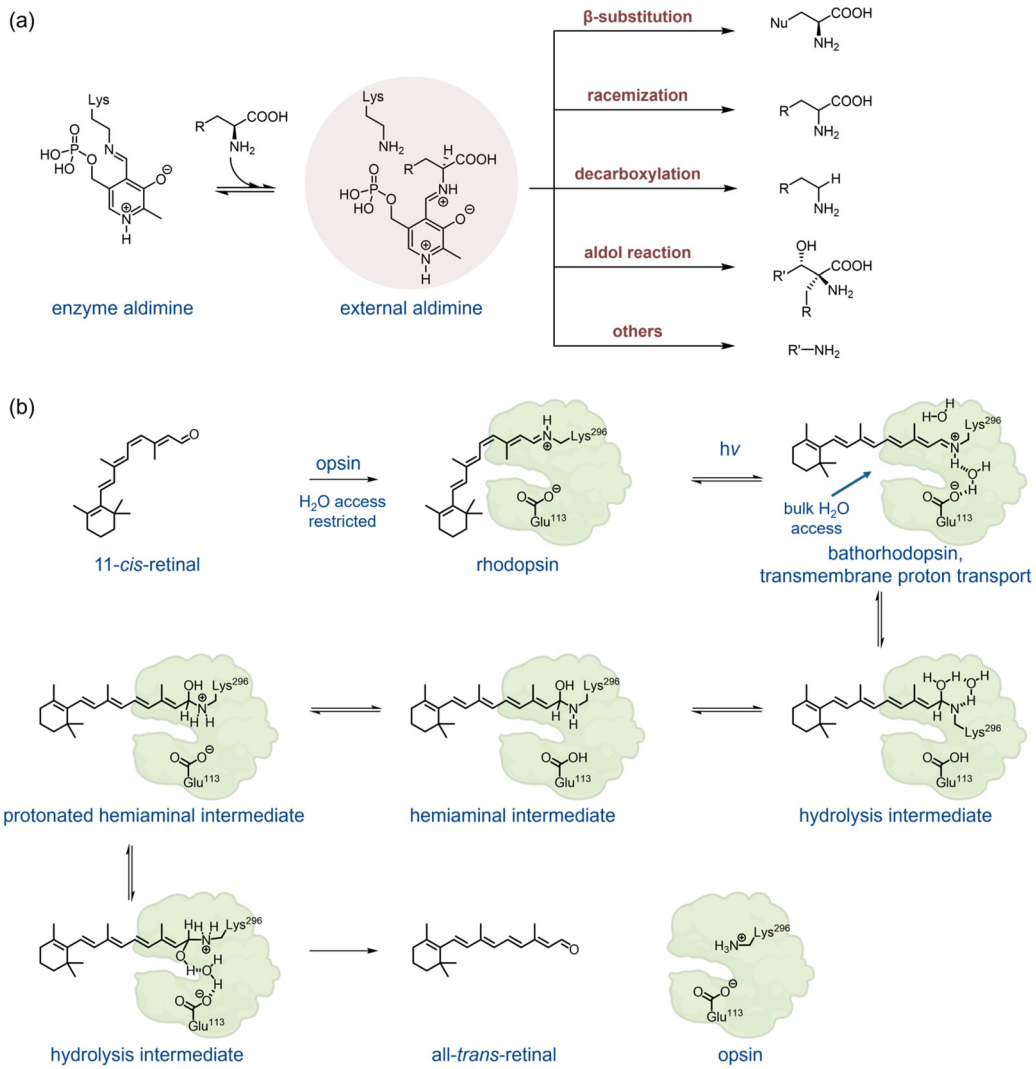

Fig. 2 (a) Summary of enzyme catalyzed transformations that use PLP as a cofactor.[19] (b) Stepwise mechanism for the formation and hydrolysis of rhodopsin. The 11-*cis*-retinal chromophore is covalently bonded *via* a protonated aldimine linkage to Lys296 located in a hydrophobic opsin binding pocket that is isolated from bulk water. The protonated aldimine is stabilized by a nearby anionic Glu113. Photoisomerization of rhodopsin rapidly forms bathorhodopsin whose strained structure induces an altered protein conformational change that induces proton transmembrane transport and also permits a water network to gain access to the aldimine linkage. Nucleophilic attack of the protonated aldimine by water is mediated by a series of proton transfers and produces the hemiaminal intermediate, with subsequent release of all-*trans*-retinal as the hydrolysis product and recycling of the opsin protein with a protonated Lys296 residue.

lization have been reviewed elsewhere and will not be discussed further here.[16–18]

The reversibility of Schiff base formation is seen often in biochemistry. A common example in enzymology is the use of pyridoxal 5′-phosphate (PLP) as an enzyme cofactor to catalyze a range of transformations based on different aspects of imine chemistry.[19,20] In each case, PLP initiates its function by forming a reversible aldimine linkage with the epsilon-amino group of a specific lysine residue within an enzyme active site. A subsequent transimination reaction attaches an incoming substrate amine and forms an external aldimine intermediate that can undergo different reactions followed by imine hydrolysis and release of the amine-containing reaction products (Fig. 2a).[21–23]

Another classic example of reversible imine formation in biochemistry concerns the visual pigment rhodopsin whose structure is composed of the 11-*cis*-retinal chromophore covalently linked *via* a protonated aldimine to Lys296 of the opsin transmembrane protein (Fig. 2b).[24–26] The protonated aldimine bond is encapsulated within a hydrophobic protein pocket which shields it from bulk water.[27] Furthermore, the protonated aldimine is stabilized by electrostatic interactions with nearby anionic residues in the pocket such as Glu113.[28–30] As a result the rhodopsin pigment is stable for days in the dark. Upon light activation, the linked 11-*cis*-retinal chromophore undergoes rapid photoisomerization to generate all-*trans*-retinal, which induces a change in the protein's transmembrane structure leading to translocation of protons across the membrane and generation of a transmembrane energy gradient. The protein conformational change also exposes the protonated aldimine bond to water and triggers hydrolytic release of all-*trans*-retinal. As shown in Fig. 2b there is considerable knowledge about the reaction intermediates that occur along the path to aldimine hydrolysis. Much of our understanding of imine hydrolysis within enzyme active-sites comes from computational modeling but the experimental literature also contains studies that have used X-ray diffraction and high-field NMR spectroscopy to identify hydrolysis intermediates such as the hemiaminal.[31]

These biological examples illustrate two binding strategies used by proteins for stabilization of a bonded Schiff base; (i) the surrounding protein structure can shield the encapsulated imine bond from bulk water and also control water access, and (ii) the protein pocket provides precisely aligned functionality that can stabilize reaction intermediates by forming favorable non-covalent interactions. These biological examples have motivated supramolecular chemists to develop biomimetic strategies to encapsulate, protect and stabilize an imine bond. This review first describes examples of solution-state host molecules with an anchored, inward-directed functional group that can form an imine bond inside the host cavity. Then the narrative progresses to host molecules with the capacity to non-covalently bind and protect a separate reactive imine guest molecule. This work exemplifies supramolecular encapsulation as a broad method to stabilize reactive molecular species.[32–36]

Self-inclusion host systems

The first supramolecular attempts to protect and stabilize imines involved self-inclusion host systems that were rationally designed to maintain the reactive imine group inside a protective concave cavity. The example in Fig. 3a shows a seminal 2007 study by Rebek and colleagues who designed the organic-soluble deep cavitand **H1** with an aldehyde group pointing directly into the cavitand binding cavity.[37,38] Using ^{1}H NMR spectroscopy, the researchers found that amines with small sizes and complementary shapes could bind inside the cavity, and form an imine bond with the inward-directed aldehyde group. Moreover, the observed change in NMR spectra over time showed that the condensation reaction inside the **H1** cavity first formed a stabilized hemiaminal intermediate with a half-life of ~90 minutes (Fig. 3b and c). The hemiaminal intermediate was stabilized by **H1** in two ways. First, the close proximity between the **H1** aldehyde and the cavity-bound amine guest promoted bimolecular attack to form the hemiaminal. Second, amide residues on the rim of **H1** provided stabilizing hydrogen bonds to the hemiaminal intermediate, which extended its lifetime. Computational work by Li and coworkers in 2013 used density functional theory (DFT) to model the structures along the reaction pathway.[39] They found that the pre-reaction complex amine@**H1** was pre-organized for nucleophilic attack, with the amine nitrogen located only 2.61 Å from the aldehyde carbon. The subsequent hemiaminal intermediate was calculated to be ~10.1 kcal mol^{-1} lower in free energy than amine@**H1** which is a remarkable level of intracavity stabilization because in free solution the hemiaminal intermediate is 3.2 kcal mol higher in free energy than the reactants. A large part of the hemiaminal stabilization arises

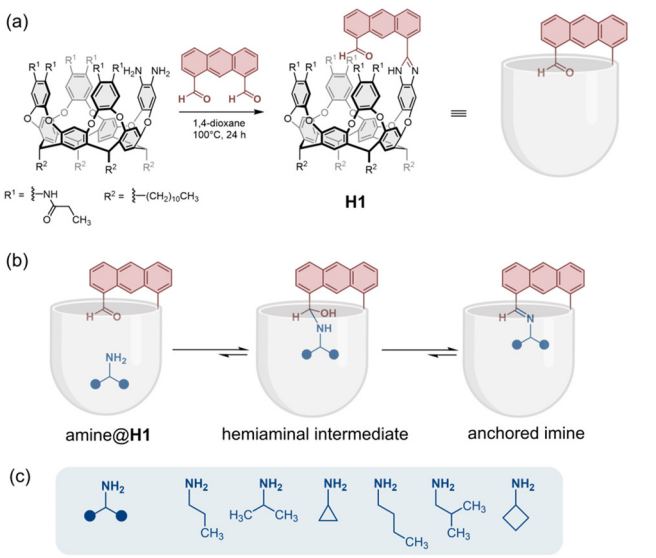

Fig. 3 (a) Synthesis of host **H1** with some peripheral groups removed for clarity. (b) NMR spectroscopy provided a rare opportunity to identify the transient hemiaminal intermediate inside host **H1**. (c) Amines for which hemiaminal formation was observed.

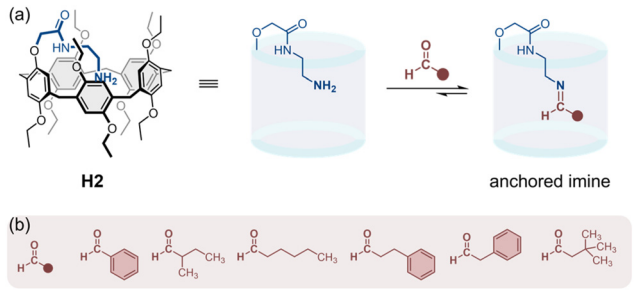

Fig. 4 (a) Chemical structure of host **H2**. (b) Chemical structures of tested aldehydes.

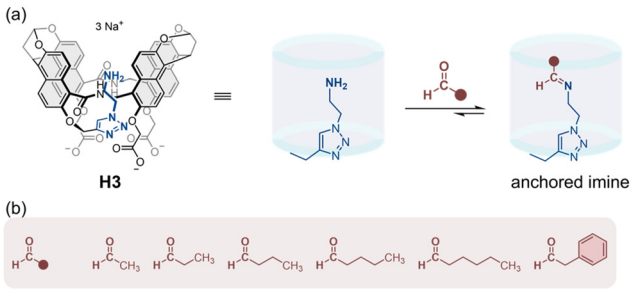

Fig. 5 (a) Chemical structure of host **H3**. (b) Chemical structures of tested aldehydes.

from hydrogen bonding with the cavitand walls. Furthermore, the rate-determining step in the entire pathway is dehydration of the hemiaminal to form the anchored imine and this step is catalyzed by proton transfer mediated by an amide NH group on the cavitand wall. Thus, several aspects of this imine-forming reaction are reminiscent of the rate enhancement factors operating in enzyme active sites.

In 2019, Yang and co-workers reported on the organic soluble pillar[5]arene host **H2** with an anchored, inward-directed aminoethyl side-chain (Fig. 4).[40] Evidence for self-inclusion was provided by NMR spectroscopy in $CDCl_3$ including NOESY spectra that showed cross-peaks between the aminoethyl side-chain and backbone protons of the pillar[5]arene. Host–guest interactions between different aldehydes and pillar[5]arene hosts were quantified by ^{1}H NMR titration, and the data showed that only small, linear aldehydes bind inside the host cavity with measurable affinity (*e.g.*, K_a = 49 M^{-1}), with essentially no binding of branched or aromatic aldehydes. Furthermore, NMR and mass spectrometry analysis showed that only the encapsulated linear aldehyde formed self-included hemiaminal or imine structures, while non-binding aldehydes did not react with the aminoethyl side-chain of the pillar[5]arene host. Control experiments with amine compounds that lacked an attached pillar[5]arene showed that the host cavity was necessary for hemiaminal or imine stabilization. The authors concluded that the hydrophobic pillar[5]arene cavity protects the reaction site by excluding water which slows hemiaminal dehydration and suppresses imine hydrolysis.

In 2022, the group of Jiang and co-workers reported a major advance by studying the water-soluble naphthotube host **H3** that is equipped an appended amine side-chain directed into the host cavity (Fig. 5a).[41] ^{1}H NMR experiments showed that adding an excess of acetaldehyde to a solution of **H3** in D_2O produced a transient set of signals corresponding to the hemiaminal intermediate and a final set of signals corresponding to the imine conjugate located inside the cavity of **H3**, a conclusion that was supported by mass spectral data. DFT calculations indicated that the hemiaminal intermediate and imine product were stabilized by hydrogen bonds with NH residues on **H3**. Longer aldehydes (Fig. 5b) had higher affinities for the hydrophobic cavity of **H3** and NMR experiments showed that they could replace the shorter acetaldehyde as an imine conjugate inside **H3**. This capacity to completely form and rapidly replace an imine bond located inside the restricted cavity of a water-soluble host is an impressive example of microenvironmental control by molecular inclusion.

In addition to the solution-state studies described above, it is worth noting that there are published reports of solid-state metal–organic frameworks with internal pore surfaces containing an amine group that can react with added low molecular weight aldehydes and form stabilized hemiaminal and imine products.[42–44]

Collectively, these self-inclusion host systems demonstrate that imine reactivity can be modulated by molecular designs that locate and orient the amine and carbonyl reactants within a microenvironment that excludes bulk water and provides non-covalent interactions to stabilize the hemiaminal intermediate and imine product. The obvious limitation with a self-inclusion host system is the requirement that one of the reactants be covalently anchored to the host, which restricts the range of potential applications.

Complexation of iminium cations inside hosts

A significant advance in this research field was advent of water-soluble host molecules with the size and molecular recognition capacity to bind and protect a reactive imine guest. In 2006, Raymond and co-workers achieved success by using a self-assembled $[Ga_4L_6]^{12-}$ metallocage with high anionic charge and a hydrophobic interior (Fig. 6a).[45] The study examined iminium cations derived from pyrrolidine (a secondary amine) and various ketones and observed negligible iminium formation in neutral or basic aqueous solution. But iminium cation formation could be promoted if it was encapsulated as a guest inside the metallocage. The encapsulation process was slow on the ^{1}H NMR time-scale and the signals for an encapsulated guest were readily identified by the diagnostic upfield changes in chemical shifts. Guest "binding efficiency" values were determined by integrating the guest and host NMR peaks and there was a dependence on the iminium cation structure

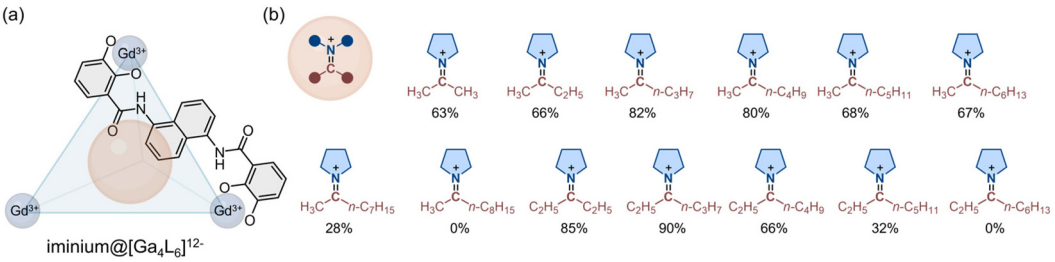

Fig. 6 (a) Stabilization of iminium ions in aqueous solution (pD 11–11.5) by molecular encapsulation within a $[Ga_4L_6]^{12-}$ metallocage. (b) Molecular recognition of iminium cations generated in water from pyrrolidine and various ketones characterized by percentage binding efficiencies which is the fraction of host molecules occupied by an iminium guest.

(Fig. 6b).[45] Moreover, it was apparent that the metallocage selected for iminium cations with a size and shape that matched with the internal volume of the metallocage. For example, iminium cations derived from acetone and 2-butanone were encapsulated with moderate binding efficiency (63–66%), whereas those derived from 3-pentanone and 3-hexanone showed nearly quantitative binding inside the metallocage (85–90%). However, no iminium cations could be observed using ketones such as 2-undecanone or 3-nonanone, as these guests were too large to fit inside the metallocage cavity. Additional experiments demonstrated that the metallocage could selectively bind a specific iminium cation out of a mixture generated from several different amines and ketones in water. In summary, the study showed that the unfavorable equilibrium for iminium cation formation in neutral or basic aqueous solution could be shifted strongly by binding the iminium cation as a guest inside a hydrophobic and polyanionic metallocage. Once captured, the iminium cation was protected from nucleophilic attack and remained stable for months at room temperature.

Cucurbit[7]uril (**CB7**) is a water-soluble host molecule with a well-known capacity to bind nitrogen-containing molecules in their protonated form. In 2017, Liu and coworkers reported that **CB7** can bind and protect complementary iminium cations in basic aqueous solution (Fig. 7a–c).[46] ^{1}H NMR spectroscopy was used to monitor the two processes of iminium hydrolysis or iminium encapsulation by **CB7** in D_2O. In the absence of **CB7** the iminium cations shown in Fig. 7c underwent very rapid hydrolysis whereas there was no measurable hydrolysis of the corresponding **CB7** : imine complex after 1 day. The NMR data was consistent with a "dynamic binding model" with either end of the imine guest protruding from the **CB7** cavity (Fig. 7a). An X-ray crystal structure provided insightful atomic detail by showing that the positively charged nitrogen atom was surrounded by the seven oxygens on the portal of **CB7**, a location that maximizes ion–dipole interactions between **CB7** and the iminium guest (Fig. 7b).

Subsequently, the same research group designed an iminium dication guest specifically tailored for the **CB7** cavity, achieving an exceptionally high binding affinity ($K_a > 10^{11}$ M^{-1}) that was driven by an optimal set of ion–dipole interactions and a perfect packing coefficient (Fig. 7d).[47] An X-ray crystal structure showed that the labile iminium bond was buried deep inside the **CB7** cavity and well protected from the aqueous environment. The complex was stable under neutral or acidic conditions, but under alkaline conditions there was release from the **CB7** host and iminium hydrolysis. The dependence of guest binding on pH was exploited to create a method for recycling **CB7** or **CB7** derivatives using the removable iminium dication guest (Fig. 7d).

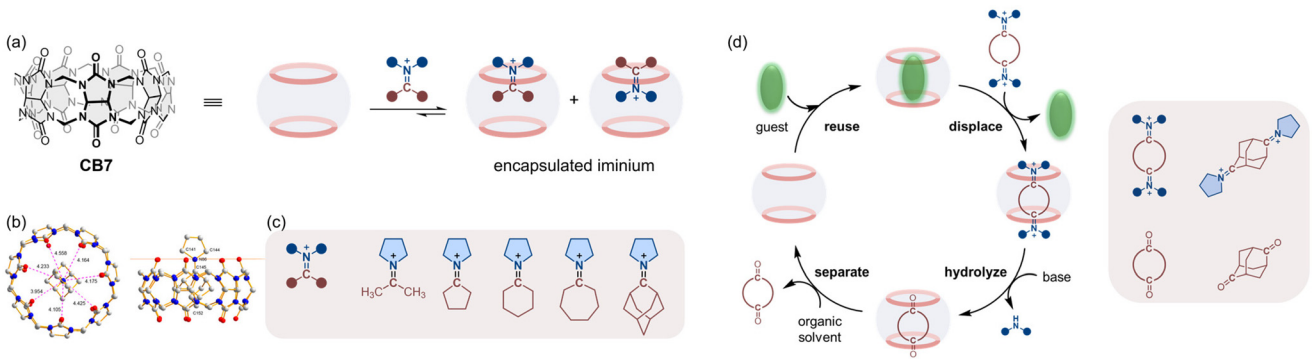

Fig. 7 (a) Structure of **CB7** and the kinetic binding model between **CB7** and iminiums. (b) Representation of the X-ray crystal structures of an iminium@**CB7** inclusion complex. (Reproduced from ref. 46 with permission from the Americal Chemical Society.) (c) Structures of iminium cations captured by **CB7** in aqueous solution. (d) Recycling of **CB7** using removable iminium dication guest.

Stabilization of Schiff bases inside hosts

Compared to the iminium cations derived from secondary amines, the imines derived from primary amines (Schiff bases) are more complex supramolecular guests because they can exist as imine bases or as protonated iminium cations with typical pK_a values in the range of 6–8. Furthermore, imine molecules containing additional functional groups can exist in different tautomeric states depending on the pH. In these cases, in change in pH can switch the structure of a host : imine complex from one that promotes imine stabilization to one that promotes imine hydrolysis.[48] This effect was demonstrated by Aliaga and colleagues who studied the impact of added **CB7** on the structure and hydrolytic stability of five different 7-diethylaminocoumarin imines with varied phenyl ring substituents.[49] Hydrolysis rates constants in acidic solution were measured using absorption spectroscopy and the kinetic data was consistent with a reaction model containing three different protonated forms of the imine substrate (free base, monoprotonated and diprotonated) and three parallel reaction pathways. In the case of 7-diethylaminocoumarin imine **IC4**, whose structure is shown in Fig. 8a, encapsulation by **CB7** to form a 1 : 1 complex led to inhibited imine hydrolysis due to complexation-induced tautomerization and formation of a less reactive structure. Formation of a 1 : 2 **IC4** : **CB7** complex (Fig. 8b) inhibited imine hydrolysis even more, an effect that was attributed to greater steric protection of the encapsulated imine. Interestingly, **CB7** complexation of two other analogous 7-diethylaminocoumarin imines produced enhanced imine hydrolysis in the acidic media, a result that was attributed to complexation-induced protonation of the imine nitrogen and imine activation for attack by water. Thus with this family of coumarin imines, complexation by **CB7** could either promote or inhibit imine hydrolysis through structure-dependent control of protonation state, tautomer distribution, or water accessibility.

While **CB7** capture of imines or oximes in weak acid leads to complexation-induced protonation of the C=N bond,[49,50] enhanced hydrolysis is not always the outcome as shown by the Smith group who demonstrated that **CB7** can complex and protect protonated Schiff bases derived from 4-(*N*,*N*-dimethylamino)benzaldehyde (Fig. 9a).[51] Absorption and NMR spectroscopy data provided clear evidence that **CB7** complexed the protonated form of these Schiff bases and greatly inhibited hydrolysis. Furthermore, addition of the high-affinity guest adamantylamine (**ADA**) to the mixture led to Schiff base displacement from the **CB7** host and immediate hydrolysis in the weak acid. A detailed subsequent investigation examined the ten different Schiff bases that are illustrated in Fig. 9b. Hydrolysis rate measurements at pH 6.0 showed that a low concentration of **CB7** could slow hydrolysis by factors up to 97-fold. The protection effect was unique to the **CB7** structure because there was no measurable protection when the Schiff bases were mixed with β-cyclodextrin, a widely used container molecule with similar cavity size as **CB7**. A combination of experimental spectroscopic data and computer modelling (quantum chemistry and molecular dynamics simulation) produced a visual and energetic rationale for the complexation and imine protection. In short, an encapsulated protonated imine is "clamped" inside the **CB7** cavity by a combination of attractive van der Waals interactions with the **CB7** interior and specific directional bonds to **CB7** oxygen atoms at each portal; specifically, a NH···O hydrogen bond between the iminium NH and an oxygen within the bottom portal, and a set of weak CH···O interactions between the *N*,*N*-dimethylamino hydrogens and the oxygens within the top portal. This "clamping" effect constrains the mobility of the encapsulated protonated imine within the **CB7** cavity and reduces its transient exposure to nucleophilic attack by the surrounding water.

Although **CB7** can capture and stabilize a pre-formed iminium cation in water, it is worth noting that there is no report of **CB7** promoting imine formation in water. Indeed, there is literature evidence for the opposite effect. For

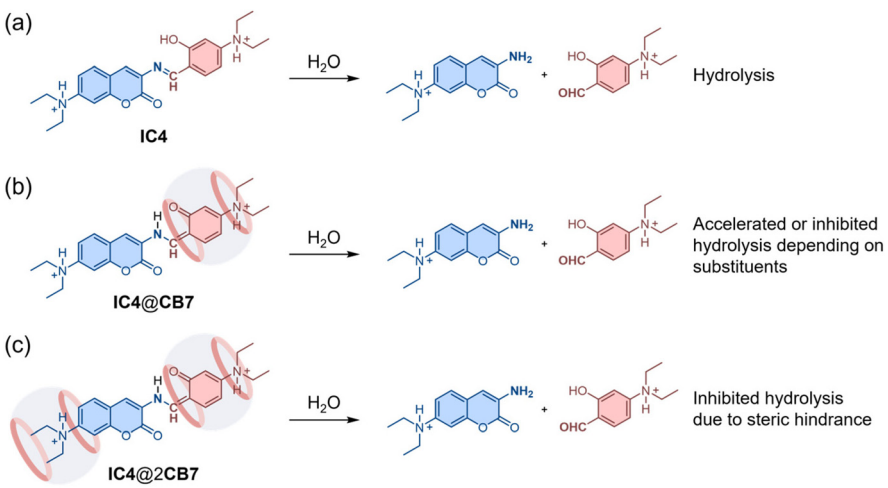

Fig. 8 Effects of **CB7** complexation on hydrolysis of the representative coumarin imine **IC4**.

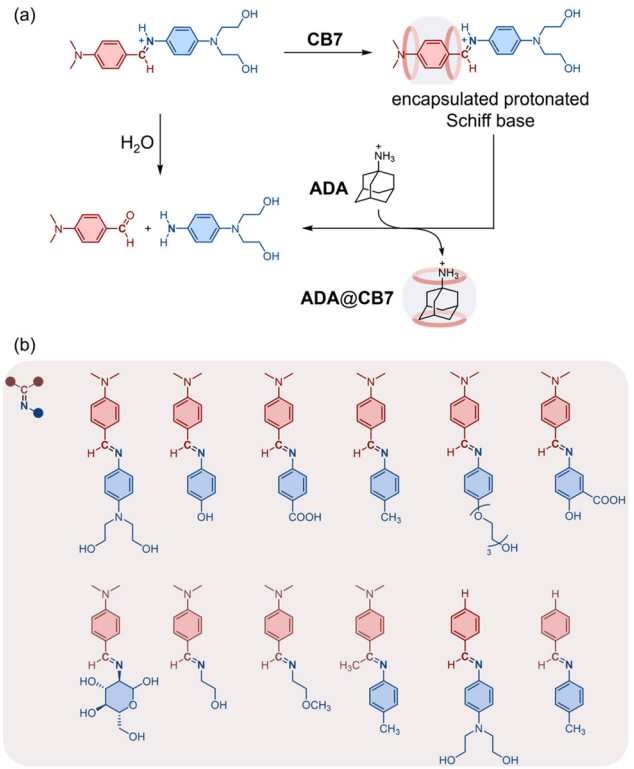

Fig. 9 (a) Chemical summary of hydrolysis, capture and protection of a protonated aldimine by **CB7**, and displacement by the competing guest **ADA**. (b) Structures of the aldimines and ketimine tested in hydrolysis studies.

example, Liu and coworkers found that a binary mixture of benzylamine and benzaldehyde at pD 9.6 produces an imine in 35% yield, but a 1 : 1 : 1.1 mixture of benzylamine : benzaldehyde : **CB7** does not produce any aldimine.[46] NMR studies of this mixture showed that the **CB7** host binds and sequesters the reactant molecules in separate complexes (especially benzylammmonium cation) and prevents them from reacting. Similarly, the presence of **CB7** does not promote the reaction of secondary amines with carbonyls in water to form iminium cations.[46]

There are two major reasons why the two host systems mentioned in this section, $[Ga_4L_6]^{12-}$ metallocage and **CB7**, do not promote an imine-forming reaction inside the host cavity. First, the host cavity sizes are not large enough to simultaneously accommodate both reactants (free amine and carbonyl) as free species, and second the electrostatic preference of both hosts is to bind amines as protonated ammonium cations, which means they cannot attack any putative co-encapsulated carbonyl. Overcoming these two problems requires a water-soluble host molecule with a cavity that is, (i) large enough to capture both reactants, and (ii) has an electrostatic preference to capture the amine as its free base. These days, the easiest way to fabricate a very large host molecule is to self-assemble a metallocage with suitably designed building blocks.[52] A relevant example is the work of Yoshizawa and colleagues who prepared a water-soluble $[Pt_2L_4]^{4+}$ metallocage with a spherical polyaromatic shell and twelve hydrophilic side-chains. The water-soluble capsule provides a closed, hydrophobic cavity with a diameter of ~1 nm and it was found to capture and protect an aldimine from hydrolysis in water at neutral pH.[53] It appears that this metallocage system was never tested for its capacity to promote imine formation in water, but high feasibility is suggested by the success described in the next paragraph.

Recently, Rebek and colleagues reported a self-assembled, dynamic capsule that was formed by spontaneous dimerization of the water-soluble cavitand **H4** (Fig. 10a). The capsule assembly is maintained by reversible Se–N chalcogen bonds and it is large enough to accommodate two guest moleules.[54] Unlike their previously studied hydrogen-bonded capsules that

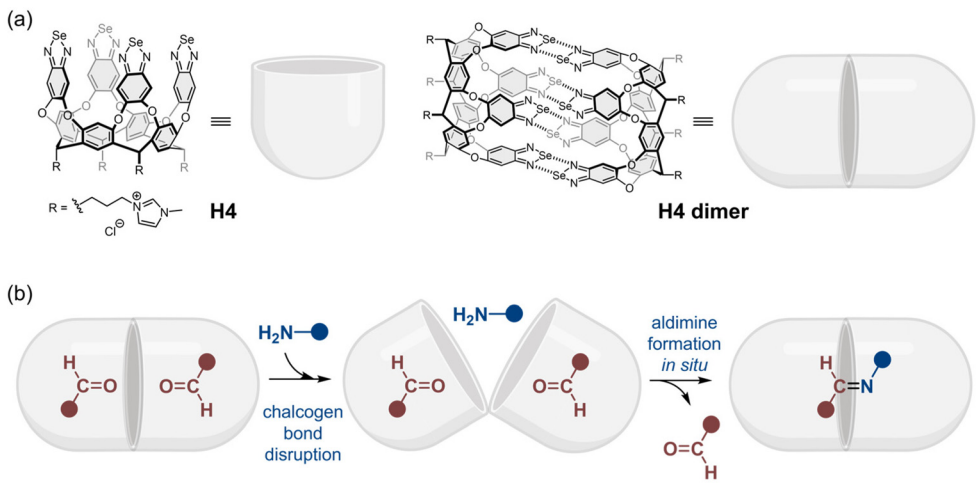

Fig. 10 (a) Cavitand **H4** dimerizes to form a capsule that is held together by multiple chalcogen bonds. (b) Proposed mechanism of aldimine formation in the **H4** dimer capsule. Free amine from the bulk solution can disrupt the chalcogen bonds at the **H4** dimer interface, and gain access to an encapsulated aldehyde to form an encapsulated aldimine, with ejection of the second aldehyde that was also in the capsule.

were permeated by water, the chalcogen-bonded interface creates a hydrophobic cavity that can capture amine and aldehyde reactants from bulk water and promote aldimine formation inside the capsule with >90% yield and a storage stability of >1 month. It was observed that aliphatic aldimines are favored over aromatic analogues because the increased flexibility of an aliphatic chain improves packing within the capsule cavity. Experiments also showed that addition of the high-affinity guest, **ADA**, could displace an aldimine from the interior of the capsule into the bulk aqueous where it was rapidly hydrolyzed.

Two possible mechanisms were contemplated for the aldimine formation reaction. In one scenario, a free amine and aldehyde react in the bulk aqueous solution to produce an aldimine that is subsequently captured by an **H4** dimer. However, this process was deemed unlikely with high-affinity hydrophobic aldehydes that could not be detected outside the capsulate. A second, more likely mechanism starts with the pre-assembly of two aldehydes inside an **H4** dimer capsule. A subsequently added free amine disrupts the chalcogen bonding at the dimer interface, leading to exposure of the encapsulated aldehyde and subsequent reaction to form an aldimine which is captured inside the capsule (Fig. 10b). This second mechanism was supported by the results of test reactions that were monitored by ^{1}H NMR. A lower concentration of free amine disproportionately slowed the imine formation, while addition of Et_3N significantly accelerated the formation, suggesting that the free amine is essential for the formation of aldimine within the host. However, aldimines only formed with amines that possessed the complementary size and shape to fit inside the container.

Future directions

Although the imine bond is quite strong, its formation in water and room temperature is a reversible equilibrium that can be controlled by the surrounding microenvironment which in turn can be modulated by supramolecular encapsulation. Over the last two decades, the supramolecular community has developed an increasingly sophisticated set of synthetic host molecues for imine complexation and stabilization, as well as strategies to trigger imine release and rapid hydrolysis. These processes can be exploited to develop kinetic traps and gatekeeping mechanisms that permit non-equilibrium chemistry.[48] By stabilizing reactive imines and iminium cations, future researchers can investigate new modes of chemical regulation and metabolic-like reaction networks.

In the near-term, different technical fields are likely to employ supramolecular strategies for controlling imine reactivity. Biomedical researchers will continue to develop new supramolecular methods for enhanced bioconjugation and drug delivery. For example, supramolecular encapsulation can be used to stabilize imine containing prodrugs or drug delivery vehicles for controlled release or selective drug activation at the site of disease. Material science is another technical field that will benefit from supramolecular-regulated imine chemistry. Prototype imine-based polymers and hydrogels have already shown great promise as self-healing and recyclable materials. By integrating host–guest regulation, new composite materials can be designed to respond to specific external triggers, such as pH changes or guest displacement.

Further into the future is the development of new supramolecular catalysts based on selective imine reaction inside a container molecule. An inspiring example of this concept is a recent publication using the self-assembled $[Ga_4L_6]^{12-}$ metallocage to catalyze several different types of chemical reactions inside the cavity, including imine reduction.[55] One example reaction is a reductive amination that selectively modifies the epsilon-amine on a protein lysine residue in preference to reaction with the protein's N-terminal amine. The reaction occurs inside the metallocage cavity where a penetrating lysine aldimine group is reduced by a co-encapsulated borane reagent. This arrangement is suggestive of the PLP-based chemistry that is mentioned in the introduction. Indeed, there is a long history going back many decades of biomimetic PLP chemistry based on supramolecular conjugates with appended PLP homologues.[20,56] Recent years has seen the advent of *endo*-functionalized metallocages that have catalytic functionality located inside the host cavity.[57,58] It seems likely that metallocages will soon be devised with an internal PLP homologue that can catalyze some of the chemical processes shown in Fig. 2a. These reactions progress through a transient imine intermediate but they release an amine-containing product that is structurally quite different. Therefore, it might be possible to minimize product inhibition with the these PLP-mimetic reactions and generate high catalytic turnover – a catalyst performance feature that has rarely been achieved using supramolecular catalysts in water.[59,60]

Conflicts of interest

There are no conflicts to declare.

Data availability

No primary research results, software or code have been included and no new data were generated or analysed as part of this review.

Acknowledgements

This work was supported by the US NSF (CHE2400154).

References

1 T. Tidwell, *Angew. Chem., Int. Ed.*, 2008, **47**, 1016–1020.
2 S. J. Rowan, S. J. Cantrill, G. R. L. Cousins, J. K. M. Sanders and J. F. Stoddart, *Angew. Chem., Int. Ed.*, 2002, **41**, 898–952.

3 M. E. Belowich and J. F. Stoddart, *Chem. Soc. Rev.*, 2012, **41**, 2003.
4 R. W. Layer, *Chem. Rev.*, 1963, **63**, 489–510.
5 K. Koehler, W. Sandstrom and E. H. Cordes, *J. Am. Chem. Soc.*, 1964, **86**, 2413–2419.
6 J. M. Sayer, M. Peskin and W. P. Jencks, *J. Am. Chem. Soc.*, 1973, **95**, 4277–4287.
7 Y. Jin, Q. Wang, P. Taynton and W. Zhang, *Acc. Chem. Res.*, 2014, **47**, 1575–1586.
8 P. Kovaříček and J.-M. Lehn, *J. Am. Chem. Soc.*, 2012, **134**, 9446–9455.
9 C.-Y. Wang, G. Wu, T. Jiao, L. Shen, G. Ma, Y. Pan and H. Li, *Chem. Commun.*, 2018, **54**, 5106–5109.
10 M. Zheng, Y. Wang, D. Hu, M. Tian, Y. Wei and J. Yuan, *Aggregate*, 2024, **5**, e624.
11 A. Aguanell, M. Hennebelle, M.Á Ortega and R. Pérez-Fernández, *Chem. Soc. Rev.*, 2025, **54**, 7093–7113.
12 S. Cambray and J. Gao, *Acc. Chem. Res.*, 2018, **51**, 2198–2206.
13 J. Weaver, G. B. Craven, L. Tram, H. Chen and J. Taunton, *J. Am. Chem. Soc.*, 2024, **146**, 24233–24237.
14 C. B. Minkenberg, L. Florusse, R. Eelkema, G. J. M. Koper and J. H. Van Esch, *J. Am. Chem. Soc.*, 2009, **131**, 11274–11275.
15 F. Liu, N. Anton, Y. Niko and A. S. Klymchenko, *ACS Appl. Bio Mater.*, 2023, **6**, 246–256.
16 S. Chatterjee, E. V. Anslyn and A. Bandyopadhyay, *Chem. Sci.*, 2021, **12**, 1585–1599.
17 Y. Chen, H. Tang, H. Chen and H. Li, *Acc. Chem. Res.*, 2023, **56**, 2838–2850.
18 M. S. Ahamed, C. Tang, S. Liu, B. Li, E. Assadpour, S. M. Jafari and Y. Li, *Adv. Colloid Interface Sci.*, 2026, **347**, 103711.
19 E. E. Snell and S. J. Di Mari, in *The Enzymes*, ed. P. D. Boyer, Academic Press, 1970, vol. 2, pp. 335–370.
20 X. Xiao and B. Zhao, *Acc. Chem. Res.*, 2023, **56**, 1097–1117.
21 R. Percudani and A. Peracchi, *EMBO Rep.*, 2003, **4**, 850–854.
22 A. Mozzarelli and S. Bettati, *Chem. Rec.*, 2006, **6**, 275–287.
23 M. D. Toney, *Arch. Biochem. Biophys.*, 2005, **433**, 279–287.
24 G. Wald, *Science*, 1968, **162**, 230–239.
25 K. Palczewski, *Annu. Rev. Biochem.*, 2006, **75**, 743–767.
26 J. D. Hong, D. Salom, M. A. Kochman, A. Kubas, P. D. Kiser and K. Palczewski, *Proc. Natl. Acad. Sci. U. S. A.*, 2022, **119**, e2213911119.
27 L. Zhu, G.-F. Jang, B. Jastrzebska, S. Filipek, S. E. Pearce-Kelling, G. D. Aguirre, R. E. Stenkamp, G. M. Acland and K. Palczewski, *J. Biol. Chem.*, 2004, **279**, 53828–53839.
28 V. Buss, M. Sugihara, P. Entel and J. Hafner, *Angew. Chem., Int. Ed.*, 2003, **42**, 3245–3247.
29 Y. Furutani, M. Shibata and H. Kandori, *Photochem. Photobiol. Sci.*, 2005, **4**, 661–666.
30 S. Sekharan, V. L. Mooney, I. Rivalta, M. A. Kazmi, M. Neitz, J. Neitz, T. P. Sakmar, E. C. Y. Yan and V. S. Batista, *J. Am. Chem. Soc.*, 2013, **135**, 19064–19067.
31 A. Heine, G. DeSantis, J. G. Luz, M. Mitchell, C.-H. Wong and I. A. Wilson, *Science*, 2001, **294**, 369–374.
32 A. Galan and P. Ballester, *Chem. Soc. Rev.*, 2016, **45**, 1720–1737.
33 B. Tang, J. Zhao, J.-F. Xu and X. Zhang, *Chem. – Eur. J.*, 2020, **26**, 15446–15460.
34 K. Wang, J. H. Jordan, X.-Y. Hu and L. Wang, *Angew. Chem., Int. Ed.*, 2020, **59**, 13712–13721.
35 K. Droguett, G. E. Quintero, J. G. Santos and M. E. Aliaga, *J. Inclusion Phenom. Macrocyclic Chem.*, 2023, **103**, 1–20.
36 R. Wang, Y. Liang, J. Rebek and Y. Yu, *Chin. Chem. Lett.*, 2024, **35**, 109228.
37 T. Iwasawa, R. J. Hooley and J. Rebek, *Science*, 2007, **317**, 493–496.
38 R. J. Hooley, T. Iwasawa and J. Rebek, *J. Am. Chem. Soc.*, 2007, **129**, 15330–15339.
39 L. Xu, S. Hua and S. Li, *Chem. Commun.*, 2013, **49**, 1542–1544.
40 X.-S. Du, Q. Jia, C.-Y. Wang, K. Meguellati and Y.-W. Yang, *Chem. Commun.*, 2019, **55**, 5736–5739.
41 M. Li, Y. Dong, M. Quan and W. Jiang, *Angew. Chem., Int. Ed.*, 2022, **61**, e202208508.
42 T. Haneda, M. Kawano, T. Kawamichi and M. Fujita, *J. Am. Chem. Soc.*, 2008, **130**, 1578–1579.
43 T. Kawamichi, T. Haneda, M. Kawano and M. Fujita, *Nature*, 2009, **461**, 633–635.
44 W. Morris, C. J. Doonan and O. M. Yaghi, *Inorg. Chem.*, 2011, **50**, 6853–6855.
45 V. Dong, D. Fiedler, B. Carl, R. Bergman and K. Raymond, *J. Am. Chem. Soc.*, 2006, **128**, 14464–14465.
46 W. Gong, J. Ma, Z. Zhao, F. Gao, F. Liang, H. Zhang and S. Liu, *J. Org. Chem.*, 2017, **82**, 3298–3301.
47 T. He, X. Hu and S. Liu, *Org. Lett.*, 2023, **25**, 246–250.
48 M. P. Van Der Helm, G. Li, M. Hartono and R. Eelkema, *J. Am. Chem. Soc.*, 2022, **144**, 9465–9471.
49 J. J. Alcázar, N. Geue, V. Valladares, A. Cañete, E. G. Pérez, L. García-Río, J. G. Santos and M. E. Aliaga, *ACS Omega*, 2021, **6**, 10333–10342.
50 C. Klöck, R. N. Dsouza and W. M. Nau, *Org. Lett.*, 2009, **11**, 2595–2598.
51 K. Shi and B. D. Smith, *Org. Biomol. Chem.*, 2025, **23**, 2606–2609.
52 A. J. McConnell, *Chem. Soc. Rev.*, 2022, **51**, 2957–2971.
53 M. Yuasa, R. Sumida, Y. Tanaka and M. Yoshizawa, *Chem. – Eur. J.*, 2022, **28**, e202104101.
54 Y. Gao, Y. Zhu, M. Zhao, J. Rebek and Y. Yu, *J. Am. Chem. Soc.*, 2025, **147**, 12989–12995.
55 M. Morimoto, W. Cao, R. G. Bergman, K. N. Raymond and F. D. Toste, *J. Am. Chem. Soc.*, 2021, **143**, 2108–2114.
56 Y. Xie, H. Pan, M. Liu, X. Xiao and Y. Shi, *Chem. Soc. Rev.*, 2015, **44**, 1741–1748.
57 C. M. Brown, D. J. Lundberg, J. R. Lamb, I. Kevlishvili, D. Kleinschmidt, Y. S. Alfaraj, H. J. Kulik, M. F. Ottaviani, N. J. Oldenhuis and J. A. Johnson, *J. Am. Chem. Soc.*, 2022, **144**, 13276–13284.
58 M. Otte, *Eur. J. Org. Chem.*, 2023, e202300012.
59 D. Zhang, L. Wang, W. Wu, D. Cao and H. Tang, *Chem. Commun.*, 2025, **61**, 599–611.
60 R. Ning and Q.-Q. Wang, *Chem. Soc. Rev.*, 2025, **54**, 11105–11140.